Self-Scheduling Models of a CAES Facility Under Uncertainties

Matheus F. Zambroni de Souza, Claudio A. Cañizares, *Fellow, IEEE*, and Kankar Bhattacharya, *Fellow, IEEE*

***Abstract*—This paper presents two mathematical formulations to represent uncertainties in self-scheduling models of a price-taker Compressed Air Energy Storage (CAES) facility. The proposed model is from the point of view of the plant owner participating in the energy, spinning, and idle reserve markets. The first described formulation is based on Robust Optimization (RO) and the second one is based on Affine Arithmetic (AA) techniques, which are both range arithmetic methodologies, and consider the thermodynamic characteristics of the CAES facility for a more realistic representation. The implementation of both methods are tested, validated and compared with each other and with Monte Carlo Simulations (MCS) using prices from the Ontario market. From the simulation results, it can be observed that both methods have some similarities, presenting lower computational burden compared with MCS, and demonstrate the advantage of applying the proposed models for CAES plant owners to hedge against price uncertainties.**

***Index Terms*—Affine Arithmetic (AA), compressed air energy storage (CAES), price uncertainties, robust optimization (RO), self-scheduling.**

NOMENCLATURE

Indices

0	Center value.
h	Noise terms.
s	Segment.
t	Operation intervals from 1 to T.

Parameters

$ang_s^{D/H}$	Slope of the Discharged Power/Heat Rate function at segment s.
$\overline{b}^D$	Length of each segment (MW).
$\overline{CA}$	Max. mass of air the cavern can store (kg).
$\overline{\Delta\pi}$	Max. price mismatch (%).
$\underline{D}_s$	Min. air discharged for segment s (kg/s).
Γ	Budget of uncertainty.
HR^n	Nominal heat rate of the facility (GJ/MWh).
M	Large number, for the Big M method.
$\underline{NG}_s$	Min. heat rate of the facility for segment s (MBTU/h).
π_t^Y	Price of Y, i.e., energy E, spinning SR and idle ID reserve, at time t ($/MWh).
π^{NG}	Price of natural gas ($/MBTU).
$\underline{P}^{C/D}, \overline{P}^{C/D}$	Charging/Discharging min. and max. limits of the CAES facility (MW).
q_s	Min. power discharged for segment s (MW).
QSC	Quick start capacity of the facility (MW).
$\underline{SOC}, \overline{SOC}$	Min. and max. limits for the State Of Charge (%).
SOC^f	Final State of Charge (%).
$VOM^{c/e}$	Variable operation and maintenance cost of the compressor c or expander e ($/MWh).

Variables

A	Revenue from energy arbitrage ($/h).
$air^{C/D}$	Amount of air charged/discharged (kg/s).
α^Y	Dual variables.
B	Revenue from spinning reserve ($/h).
b_s^D	Fractional value of segment s (MW).
CO^{NG}	Cost of natural gas ($/h).
$\Delta\pi^Y$	Price deviation of Y (%).
$\Delta\pi^{Y+/-}$	Upward/Downward price deviation of Y (%).
ε^Y	Noise term of Y.
OC	Operation cost ($/h).
P^X	Power in X mode, i.e., discharging D, charging C, spinning reserve discharging SRD, spinning reserve charging SRC or idle ID (MW).
SOC	State Of Charge (%).
u_s^D	Binary variable to identify the operating segment s.
w	Variable used to linearize bi-linear terms.
$x^{C/D}$	Binary variable indicating Charging/Discharging mode.
$\hat{\cdot}$	Affine representation of an uncertain variable.

Functions

$AFR^C(SOC)$	Charging air flow rate as a function of the SOC ($kg.MW^{-1}.s^{-1}$).
$AFR^D(P^D)$	Discharging air flow rate as a function of P^D ($kg.MW^{-1}.s^{-1}$).
$f(P^X)$	Revenue equation as a function of the power dispatch ($/h).
$HR(P^D)$	Heat rate as a function of P^D (GJ/MWh).
$\mathcal{F}$	Objective function.

Manuscript received July 14, 2020; revised November 16, 2020 and December 28, 2020; accepted January 2, 2021. Date of publication January 6, 2021; date of current version June 18, 2021. This work was supported in part by the Natural Sciences, and Engineering Research Council of Canada (NSERC), under Grant CRDPJ 477323 - 14, and in part by the Ontario Centres of Excellence (OCE). Paper no. TPWRS-01173-2020. *(Corresponding author: Claudio Canizares.)*

The authors are with the Department of Electrical, and Computer Engineering, University of Waterloo, Waterloo, ON N2L 3G1, Canada (e-mail: m6ferrei@uwaterloo.ca; ccanizar@uwaterloo.ca; kankar@uwaterloo.ca).

Color versions of one or more figures in this article are available at https://doi.org/10.1109/TPWRS.2021.3049742.

Digital Object Identifier 10.1109/TPWRS.2021.3049742

I. Introduction

POWER systems are faced with the challenge of maintaining demand-supply balance while operating under secure conditions, i.e., maintaining voltages and frequency within limits and ensuring stability [1]. With the increasing penetration of intermittent Renewable Energy Sources (RES) in recent years, new challenges have come to the fore in power system operation. To tackle these challenges, Energy Storage Systems (ESS) are being deployed for various applications such as energy arbitrage, peak shaving, and others [2]. Thus, ESS facilities can either be an asset of the system or owned by a private investor and it can operate either as a price-taker or price-maker, depending on its capacity compared to the system capacity [3]. From the owner's point of view, one of its main challenges is to obtain the optimum schedule that maximizes its daily profit. In this context, a novel Battery Energy Storage System (BESS) operational cost structure, considering its degradation cost is proposed in [4], presenting a market auction model for these types of facilities assuming that they participate and bid in energy and spinning reserve markets. A study evaluating non-strategic (price-taker) and strategic (price-maker) participation of a Pumped Hydro Storage (PHS) in energy and performance-based regulation market is proposed in [5], considering uncertainties on demand and competitors' offers, and assuming that the facility can charge and discharge simultaneously.

Of the existing ESS technologies, Compressed Air Energy Storage (CAES) is one of the most appropriate for bulk power system applications [6], with two large CAES facilities existing in the world [6], [7]. However, despite being a known technology that is being actively considered for wider deployment [8], not many studies on their operation in electricity markets are reported. In [9], a mathematical model for the representation of CAES systems in steady-state and dynamic studies is presented. A self-scheduling model to maximize the daily profit of a CAES facility, considering its thermodynamic characteristics is presented in [10]; however, the work does not take into consideration the presence of uncertainties. A risk-constrained bidding and offering strategy for a CAES facility using information gap decision theory is proposed in [11], while [12] proposes a Robust Optimization (RO) approach to obtain the optimal bids and offers and a robust self-scheduling model for a wind producer paired with a CAES system is proposed in [13]. Despite presenting uncertainty immunized solutions in [11]–[13], the CAES model used do not consider minimum charge and discharge limits nor the CAES thermodynamic characteristics, and the facility is assumed to participate only in the energy market.

Uncertainties in load and RES generation have been an issue for power systems operation. Thus, in [14], a chance-constrained unit commitment (UC) model considering wind uncertainty is presented. A stochastic Local Marginal Price (LMP) market model considering uncertainties in wind power generation is proposed in [15]. Both [14] and [15] represent uncertainties using probability density functions (pdfs), which despite being robust, have non-linear characteristics and require large amounts of data to achieve accurate representations, with lack of data resulting in assumptions that lead to poor results [16]. Hence, to avoid the use of pdfs, methods based on range arithmetic, such as RO and Affine Arithmetic (AA) have been proposed in the literature.

An energy management system for isolated microgrids using RO is proposed in [16], representing the uncertainties in wind power generation, while reducing load interruptions and increasing energy reserves. An algorithm to obtain the optimum hourly bid/offer prices for a price-maker ESS facility using RO, considering uncertainties in demand and supply curves, is proposed in [17]; the authors conclude that the proposed approach provides a higher level of financial protection when compared to a risk-neutral strategy.

An AA-based methodology for power flow analysis considering uncertainties is proposed in [18], where it is shown that despite the method being more conservative than the Monte Carlo Simulation (MCS) approach, it presents lower computational burden and can be applied to large-scale systems. In [19], the authors apply AA to solve the optimum power flow problem with uncertainties in RES generation; benchmarked with MCS, the method is shown to have much lower computational costs, and yields similar results for both small and large systems. An UC problem using the AA method is introduced in [20], considering uncertainties in demand and RES generation, demonstrating that it provides robust results at a reasonable computational burden.

Even though both RO and AA methods are based on range arithmetic, only a few studies have been published in the literature that explore their similarities and differences, as for example in [21], where RO and AA models minimize microgrid operating costs are proposed and compared considering uncertainties in demand and RES generation. To the best of the authors' knowledge, no works have been reported where these methods are compared in a self-scheduling model of a storage facility. Thus, two mathematical tools based on range arithmetic are explored for a self-scheduling, price-taker CAES facility model, i.e., for a small plant that does not affect the system dispatch and electricity prices, which can vary by up to 36% from their forecasted values [22]. As a market participant, the CAES facility operational strategy can be risk-averse or risk-taking; however, even though the risk-taking approach yield higher profits in an optimistic scenario, in a pessimistic scenario it can result in much lower profits, and even losses. Therefore, to ensure a safe margin of profit, the CAES facility is assumed to be risk-averse, as most market participants [23].

Based on the aforementioned discussion, the main objectives of the paper are the following:

- Present a self-scheduling model for a price-taker CAES facility participating in electricity markets, including the thermodynamic characteristics of the facility.
- Propose an RO model that considers uncertainties in prices to optimize the CAES owner's profit under the worst-case scenario.
- Propose an AA model considering uncertainties in prices to determine the dispatch schedule and profit margin of the CAES facility.
- Compare the results and performances for RO and AA models using a realistic test case.

With the main contributions being the following:

- A new formulation for representing the thermodynamic characteristics of the CAES model is proposed based on a linearization of the corresponding nonlinear functions presented in [10]. This reduces the number of binary variables in the mathematical model, thus improving the computational performance and allowing the AA based approach to keep track of correlated uncertainties.
- Novel self-scheduling mathematical models for CAES facilities are proposed based on two different uncertainty modeling approaches, namely, RO and AA, comparing them in detail. These techniques would help CAES facility owners to choose the most appropriate self-schedule taking into account price uncertainties.
- The proposed self-scheduling model considers CAES facilities participating in both energy and spinning reserve markets simultaneously, while considering uncertainties in market prices. This would allow CAES facilities to avail of greater market opportunities to improve its value stream.

The rest of the paper is organized as follows: Section II presents the deterministic mathematical model to maximize the daily profit of the CAES facility, introducing its thermodynamic characteristics. The RO and AA models are presented in Sections III and IV, respectively, and the results and comparisons for both models are presented and discussed in Section V. Finally, Section VI summarizes the main contributions and conclusions of the paper.

II. Deterministic CAES Operating Model

In this work, the CAES facility is assumed to be a price-taker, i.e., it does not affect the market price by its actions. The facility participates in the day-ahead market, providing energy, spinning and idle reserves to the power system, seeking to maximize its daily profit as follows:

$$\max_{P_t^X} \mathcal{F} = \sum_{t}^{T} \left[f(P_t^X) - OC_t \right] \tag{1}$$

where:

$$f(P_t^x) = A_t \pi_t^E + B_t \pi_t^{SR} + P_t^{ID} \pi_t^{ID} \qquad \forall t \tag{2}$$

$$A_t = P_t^D - P_t^C \qquad \forall t \tag{3}$$

$$B_t = P_t^{SRD} + P_t^{SRC} \qquad \forall t \tag{4}$$

$$OC_t = CO_t^{NG} + P_t^D VOM^e + P_t^C VOM^c \qquad \forall t \tag{5}$$

All variables and parameters in these and other equations are defined in the nomenclature section. In (2), the first term represents the revenue from energy arbitrage, where the facility is remunerated for the energy it discharges while it pays for the energy consumed during charging, as per (3); the second and third terms denote the revenues from spinning, as per (4), and idle reserves, respectively. The operational cost is given by (5), where the first term denotes the cost of natural gas in the discharging stage, as discussed in detail later; the second term is the Variable Operational and Maintenance (VOM) cost for the expander during discharging; and the third term is the VOM cost of the compressor during charging.

The operational constraints of the CAES facility can be defined as follows:

$$x_t^C + x_t^D \leq 1 \qquad \forall t \tag{6}$$

$$P_t^C \leq \overline{P}^C x_t^C \qquad \forall t \tag{7}$$

$$\underline{P}^C x_t^C \leq P_t^C - P_t^{SRC} \qquad \forall t \tag{8}$$

$$P_t^D + P_t^{SRD} \leq \overline{P}^D x_t^D \qquad \forall t \tag{9}$$

$$\underline{P}^D x_t^D \leq P_t^D \qquad \forall t \tag{10}$$

$$0 \leq P_t^{ID} \leq QSC[1 - (x_t^C + x_t^D)] \qquad \forall t \tag{11}$$

Equation (6) constraints the CAES to operate in either charging, discharging, or idle modes. Equations (7) to (11) represent the maximum and minimum power capacities of charging, discharging, spinning, and idle reserves, respectively. The upper and lower limits of the compressor charging power must be between 40%-100% of the rated power, where its efficiency is approximately constant, whereas for the turbine limits, the discharging power must be between 30%-100% of the rated power, where its efficiency is not compromised [24].

The relationships governing the CAES facility State of Charge (SOC) and cost of natural gas are given by:

$$SOC_{t+1} = SOC_t + \frac{air_t^C 3600}{\overline{CA}} - \frac{air_t^D 3600}{\overline{CA}} \qquad \forall t \tag{12}$$

$$air_t^C = AFR^C(SOC_t) P_t^C \qquad \forall t \tag{13}$$

$$air_t^D = AFR^D(P_t^D) P_t^D \qquad \forall t \tag{14}$$

$$CO_t^{NG} = HR(P_t^D) P_t^D \pi^{NG} \qquad \forall t \tag{15}$$

$$SOC_{t+1} \geq SOC^f \qquad \forall t = T \tag{16}$$

In (12), the SOC of the cavern is calculated for time $t+1$, given the SOC and the amount of air charged or discharged at time t, which are calculated in (13) and (14), respectively, where the charging/discharging power is multiplied with the charging/discharging Air Flow Rate (AFR) of the facility. Since the facility is set to participate in the next day electricity market, the SOC is forced to be at least at the minimum limit SOC^f in (16), so that it is better prepared for the next day opportunities.

In (13), the charging AFR is a function of the SOC, since as the SOC of the cavern increases, so does the pressure, making it difficult to store more air inside the facility, thus reducing the AFR; the function $AFR^C(SOC_t)$ is illustrated in Fig. 1(a). In (14), the discharging AFR is a function of the discharged power, given as $AFR^D(P_t^D)$ and depicted in Fig. 1(b). This behavior is associated with the efficiency of the high pressure turbine reducing when the facility operates below its nominal power (below 100 MW in Fig. 1), and thus a greater AFR is necessary to generate one unit of power. Since a greater AFR is required to generate one unit of power when operating below the nominal value, more natural gas is required; thus, the Heat Rate (HR) of the facility increases for lower discharge. The function $HR(P_t^D)$ is shown in Fig. 1(c). The data illustrated in Fig. 1 was obtained from the Huntorf CAES facility in Germany [6].

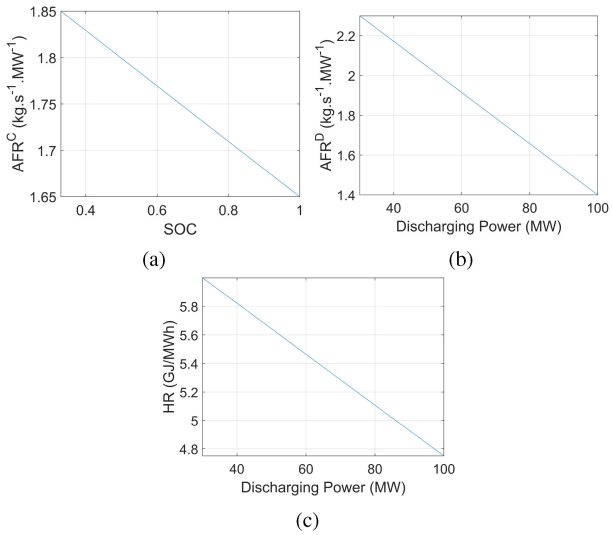

Fig. 1. CAES thermodynamic characteristics: a) AFR^C vs SOC, b) AFR^D vs Discharging power, and c) HR vs Discharging power.

The aforementioned functional relationships are represented as step functions in [10], which complicates the mathematical model, since the number of binary and auxiliary variables increases, thereby increasing the computational burden. Furthermore, when using methods that keep track of correlated uncertainties, as in the case of methodologies such as the proposed AA model, the discontinuities in the step functions increase the model complexity. Therefore, in this work, the following new approximation functions are proposed, using linear interpolations to represent the thermodynamic characteristics of the CAES facility, as shown in Fig. 1:

$$AFR^C(SOC_t) = -0.3SOC_t + 1.95 \qquad \forall t \qquad (17)$$

$$AFR^D(P_t^D) = -\frac{0.9}{70}P_t^D + \frac{18.8}{7} \qquad \forall t \qquad (18)$$

$$HR(P_t^D) = -\frac{1.25}{70}P_t^D + \frac{457.5}{70} \qquad \forall t \qquad (19)$$

Note that, since the compressor efficiency remains fairly constant in the operating range considered (40-100%), the AFR can be assumed to be a linear function of the SOC, as in (17).

Thus, the equation for the mass of air charged at time t, is given by:

$$air_t^C = -0.3\underbrace{SOC_tP_t^C}_{\text{Bi-linear term}} + 1.95P_t^C \qquad \forall t \qquad (20)$$

where the bi-linear term in (20) can be linearized to make the model a Mixed-Integer Linear Programming (MILP) problem. Thus, given the intervals of the variables, the bi-linear term can be relaxed into a set of linear constraints using McCormick Envelopes as follows [25]:

$$w_t = SOC_tP_t^C \qquad \forall t \qquad (21)$$

$$w_t \geq \underline{SOC}P_t^C + SOC_t\underline{P}^C - \underline{SOC}\,\underline{P}^C \qquad \forall t \qquad (22)$$

$$w_t \geq \overline{SOC}P_t^C + SOC_t\overline{P}^C - \overline{SOC}\,\overline{P}^C \qquad \forall t \qquad (23)$$

$$w_t \leq \underline{SOC}P_t^C + SOC_t\overline{P}^C - \underline{SOC}\overline{P}^C \qquad \forall t \qquad (24)$$

$$w_t \leq \overline{SOC}P_t^C + SOC_t\underline{P}^C - \overline{SOC}\underline{P}^C \qquad \forall t \qquad (25)$$

Hence, (20) can be reformulated as:

$$air_t^C = -0.3w_t + 1.95P_t^C \qquad \forall t \qquad (26)$$

Constraints (22)-(25) are valid when the CAES facility is charging, i.e., for P_t^C within its lower and upper limits. However, when the facility is not charging ($P_t^C = 0$) the problem becomes numerically infeasible, since (22) and (25) would force w_t to be positive and negative, respectively. Thus, the big M approach is used in the model to avoid numerical infeasibility, as follows:

$$w_t \leq Mx_t^C \qquad \forall t \qquad (27)$$

$$w_t \geq \underline{SOC}P_t^C + SOC_t\underline{P}^C - \underline{SOC}\,\underline{P}^C - M(1 - x_t^C) \qquad \forall t \qquad (28)$$

$$w_t \geq \overline{SOC}P_t^C + SOC_t\overline{P}^C - \overline{SOC}\,\overline{P}^C - M(1 - x_t^C) \qquad \forall t \qquad (29)$$

$$w_t \leq \underline{SOC}P_t^C + SOC_t\overline{P}^C - \underline{SOC}\overline{P}^C + M(1 - x_t^C) \qquad \forall t \qquad (30)$$

$$w_t \leq \overline{SOC}P_t^C + SOC_t\underline{P}^C - \overline{SOC}\underline{P}^C + M(1 - x_t^C) \qquad \forall t \qquad (31)$$

The above set of constraints ensure that when the CAES facility is not in charging mode, i.e., $w_t = 0$, no numerical infeasilibility arises from the constraints.

The relationships for the mass of air discharged and the cost of natural gas are obtained from replacing (18) and (19) in (14) and (15), respectively, as follows:

$$air_t^D = -\frac{0.9}{70}\left(P_t^D\right)^2 + \frac{18.8}{7}P_t^D \qquad \forall t \qquad (32)$$

$$\frac{CO_t^{NG}}{\pi^{NG}} = -\frac{1.25}{70}\left(P_t^D\right)^2 + \frac{457.5}{70}P_t^D \qquad \forall t \qquad (33)$$

Observe that these functions are quadratic, which can be linearized using a piece-wise linearization approach, as shown in Fig. 2. Thus, the mass of air discharged by the facility and the cost of natural gas at time t can be determined as follows:

$$P_t^D = \sum_{s=1}^{2}\left(b_{t,s}^D + \underline{q}_s u_{t,s}^D\right) \qquad \forall t \qquad (34)$$

$$\sum_{s=1}^{2} u_{t,s}^D = x_t^D \qquad \forall t \qquad (35)$$

$$0 \leq b_{t,s}^D \leq \overline{b}^D u_{t,s}^D \qquad \forall t, s \qquad (36)$$

$$air_t^D = \sum_{s=1}^{2}\left(ang_s^D b_{t,s}^D + \underline{D}_s u_{t,s}^D\right) \qquad \forall t \qquad (37)$$

$$CO_t^{NG} = \sum_{s=1}^{2}\left(ang_s^H b_{t,s}^D + \underline{NG}_s u_{t,s}^D\right)\pi^{NG} \qquad \forall t \qquad (38)$$

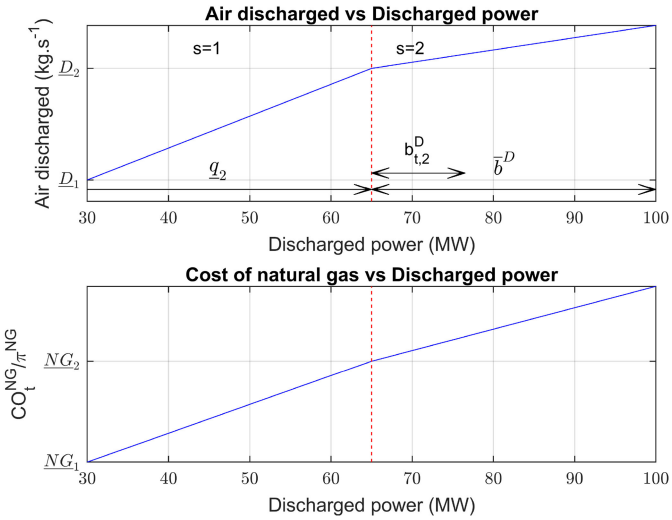

Fig. 2. Linear approximation of the quadratic functions.

where from (34) to (36), the power discharged is expressed in terms of variables and parameters that are used to identify the operating point of the CAES facility. Hence, (37) and (38) determines the air discharged and cost of natural gas, respectively.

III. RO Formulation of CAES Operations Model

In this work, since the optimization problem seeks to maximize the daily profit of a price-taker CAES facility, the main source of uncertainty are electricity prices, i.e., energy and reserve market prices. To this effect, the prices can be expressed in terms of their center values (forecast price) and the deviation from it, as follows:

$$\pi_t^Y = \pi_{0,t}^Y(1+\Delta\pi_t^Y) \qquad \forall t, Y \tag{39}$$

In the RO formulation, the objective is to maximize the profit of the facility under worst case scenarios. Thus, substituting (39) in (1), the objective function and additional constraints of the optimization problem can be stated as follows:

$$\max_{P_t^X}\min_{\Delta\pi_t^Y} \mathcal{F} = \sum_t^T \Bigg[f(P_t^X) - OC_t + \underbrace{\Delta\pi_t^E A_t}_{\text{Bi-linear term}} \pi_{0,t}^E + \underbrace{\Delta\pi_t^{SR} B_t}_{\text{Bi-linear term}} \pi_{0,t}^{SR} + \underbrace{\Delta\pi_t^{ID} P_t^{ID}}_{\text{Bi-linear term}} \pi_{0,t}^{ID} \Bigg] \tag{40}$$

where:

$$\Delta\pi_t^Y = \Delta\pi_t^{Y+} - \Delta\pi_t^{Y-} \qquad \forall t, Y \tag{41}$$

$$\Delta\pi_t^{Y+} - \overline{\Delta\pi} \le 0 \qquad \forall t, Y \tag{42}$$

$$\Delta\pi_t^{Y-} - \overline{\Delta\pi} \le 0 \qquad \forall t, Y \tag{43}$$

$$\sum_t^T \frac{\Delta\pi_t^{Y+} + \Delta\pi_t^{Y-}}{\overline{\Delta\pi}} - \Gamma \le 0 \qquad \forall Y \tag{44}$$

$$\Delta\pi_t^{Y+}, \Delta\pi_t^{Y-} \ge 0 \qquad \forall t, Y \tag{45}$$

The modified objective function (40) represents a max-min problem, where the profit is maximized in terms of power arbitrage variables and minimized in terms of price deviation. Equation (41) calculates the energy, spinning and idle reserve price deviations, and (42) and (43) limit the upward and downward deviations to their maximum allowed levels, respectively. Finally, (44) provides the flexibility of conservatism in the model through the budget of uncertainty Γ, which limits the number of times the prices deviate from their forecast values. Choosing a higher $\overline{\Delta\pi}$ provides more financial protection against larger price mismatches.

Equation (40) presents a max-min structure, which is a saddle-node problem and usually non-convex [16], including a new set of bi-linear terms that do not allow the problem to be solved as an MILP problem. Using the dual of the minimization problem (40)-(44), one has:

$$\max_{P_t^X, \alpha_{1,t}^Y - \alpha_{3,t}^Y, \alpha_4^Y} \mathcal{F} = \sum_t^T \Big[f(P_t^X) - OC_t + \overline{\Delta\pi}(\alpha_{2,t}^E + \alpha_{3,t}^E + \alpha_{2,t}^{SR} + \alpha_{3,t}^{SR} + \alpha_{2,t}^{ID} + \alpha_{3,t}^{ID}) \Big] + \left(\alpha_4^E + \alpha_4^{SR} + \alpha_4^{ID}\right)\Gamma \tag{46}$$

where:

$$\alpha_{2,t}^Y,\ \alpha_{3,t}^Y,\ \alpha_4^Y \le 0 \qquad \forall t, Y \tag{47}$$

$$\alpha_{1,t}^E = A_t \pi_{0,t}^E;$$

$$\alpha_{1,t}^{SR} = B_t \pi_{0,t}^{SR};\ \alpha_{1,t}^{ID} = P_t^{ID} \pi_{0,t}^{ID} \qquad \forall t \tag{48}$$

$$-\alpha_{1,t}^Y + \alpha_{2,t}^Y + \frac{\alpha_4^Y}{\overline{\Delta\pi}} \le 0 \qquad \forall t, Y \tag{49}$$

$$\alpha_{1,t}^Y + \alpha_{3,t}^Y + \frac{\alpha_4^Y}{\overline{\Delta\pi}} \le 0 \qquad \forall t, Y \tag{50}$$

Observe in (46) that the objective function is now a maximization problem without bi-linear terms, and hence the problem can be solved as an MILP problem.

In RO, a constraint with n uncertain parameters has a probability p of being violated, which can be determined for a given value of Γ as follows [26]:

$$p = 1 - \Phi\left(\frac{\Gamma - 1}{\sqrt{n}}\right) \tag{51}$$

where Φ is the cumulative distribution of a standard normal function. Thus, based on the results obtained and the probability of violation corresponding to Γ, the CAES facility operator can choose a schedule that ensures profit maximization while protecting it from a given level of uncertainties.

IV. AA Formulation of CAES Operations Model

A. Affine Arithmetic Overview

AA is a range analysis technique that keeps track of correlated uncertainties between the variables [27]. It handles both external and internal uncertainty sources, with imprecise data and uncertainty in the mathematical model being an external source,

and truncation and round-off errors being internal sources. Each uncertain variable χ is represented in its affine form as follows:

$$\hat{\chi} = \chi_0 + \chi_1\varepsilon_1 + \chi_2\varepsilon_2 + \cdots + \chi_p\varepsilon_p = \chi_0 + \sum_{h=1}^{p}\chi_h\varepsilon_h \quad (52)$$

where χ_0 denotes the center value of the variable χ, whereas ε_h and χ_h are the noise variables and magnitude of the corresponding uncertainty component, respectively; the noise variables are within the interval $[-1, 1]$. Hence, when all variables are represented in their affine forms, they all share the same noise variables, thus tracking correlated uncertainties.

In AA, there are affine and non-affine operations. Thus, considering the affine quantities $\hat{a} = a_0 + \sum_{h=1}^{p} a_h\varepsilon_h$ and $\hat{b} = b_0 + \sum_{h=1}^{p} b_h\varepsilon_h$ and the parameter λ, affine operations are the following:

$$\hat{z} = \hat{a} \pm \hat{b} = (a_0 \pm b_0) + \sum_{h=1}^{p}(a_h \pm b_h)\varepsilon_h \quad (53)$$

$$\hat{z} = \lambda\hat{a} = \lambda a_0 + \lambda\sum_{h=1}^{p} a_h\varepsilon_h \quad (54)$$

$$\hat{z} = \hat{a} \pm \lambda = (a_0 \pm \lambda) + \sum_{h=1}^{p} a_h\varepsilon_h \quad (55)$$

and a non-affine operation is:

$$\hat{z} = \hat{a}\hat{b} = a_0b_0 + \sum_{h=1}^{p}(a_0b_h + b_0a_h)\varepsilon_h + z_k\varepsilon_k \quad (56)$$

where the resulting variables contains the information provided by $\hat{a}$ and $\hat{b}$, and the approximation error is denoted as $z_k\varepsilon_k$. Despite being conservative, ε_k is usually assumed to be 1 and $z_k = \sum_{h=1}^{p}|a_h|\sum_{h=1}^{p}|b_h|$. Thus, (56) can be rewritten as:

$$\hat{z} = a_0b_0 + \sum_{h=1}^{p}(a_0b_h + b_0a_h)\varepsilon_h + \sum_{h=1}^{p}|a_h|\sum_{h=1}^{p}|b_h| \quad (57)$$

Optimization problems using AA can be represented in general form as follows [28]:

$$\max_{\hat{z}} \ \hat{\mathcal{F}}(\hat{z}) \quad (58)$$

$$\text{s.t. } \hat{g}_l(\hat{z}) = 0 \quad \forall l \in L \quad (59)$$

$$\hat{h}_m(\hat{z}) \le 0 \quad \forall m \in M \quad (60)$$

where equality $\hat{a} = \hat{b}$ and inequality $\hat{a} \le \hat{b}$ constraints can be respectively presented as follows:

$$a_0 = b_0 \wedge a_h = b_h \quad \forall h \quad (61)$$

$$a_0 + \sum_{h=1}^{p}|a_h| \le b_0 - \sum_{h=1}^{p}|b_h| \quad (62)$$

with (61) stating that one affine variable is equal to the other if all their terms are equal, and (62) indicating that one affine variable is less than the other if the upper boundary of the left-hand side is less than the lower boundary of the right-hand side.

Since the objective function (58) can be expanded as follows:

$$\max_{\hat{z}} \hat{\mathcal{F}}(\hat{z}) = \mathcal{F}_0(\hat{z}) + \sum_{h=1}^{p}\mathcal{F}_h(\hat{z})\varepsilon_h + \sum_{h=p+1}^{p+p_{na}}\mathcal{F}_h(\hat{z})\varepsilon_h \quad (63)$$

it is shown in [28] that this can be represented as the following multi-objective problem:

$$\max_{\hat{z}} \left\{\mathcal{F}_0(\hat{z}), \sum_{h=1}^{p+p_{na}}|\mathcal{F}_h(\hat{z})|\right\} \quad (64)$$

where the first term is denoted as the center, and the second term is denoted as the radius from the center to the boundaries of the objective function. Thus, (64) essentially allows maximizing the center value (deterministic problem) or the radius of the objective function (uncertain problem).

B. AA Model of the CAES Facility

As previously mentioned, for a price-taker CAES facility, the main source of uncertainties are the electricity prices, which can be expressed in their affine forms as follows:

$$\hat{\pi}_t^Y = \pi_{0,t}^Y(1 + \varepsilon_t^Y\overline{\Delta\pi}) \quad \forall t, Y \quad (65)$$

And the power dispatch variables can be expressed as follows:

$$P_t^X = P_{0,t}^X + P_{1,t}^X\varepsilon_t^E + P_{2,t}^X\varepsilon_t^{SR} + P_{3,t}^X\varepsilon_t^{ID} \quad \forall t, X \quad (66)$$

Equation (64) can be maximized using a decoupled approach, i.e., maximize the center and radius of the objective function separately; however, this is valid for a problem with continuous variables only. Hence, since the CAES model has binary variables x_t^C and x_t^D and inter-temporal constraints (12), it cannot be guaranteed that the solution of one maximization would be feasible for the other [20]. Therefore, the objective function be re-formulated as follows:

$$\max_{\hat{P}_t^X} \sum_{t=1}^{T}\left(\mathcal{F}_0(\hat{P}_t^X) + \sum_{h=1}^{p}|\mathcal{F}_h(\hat{P}_t^X)| - \sum_{h=p+1}^{p_{na}}|\mathcal{F}_h(\hat{P}_t^X)|\right) \quad (67)$$

where the center and radius are maximized simultaneously, while the non-affine radius is minimized to reduce the conservatism of the process, obtaining a single and a reasonably conservative result for the optimum daily schedule of the CAES facility, which can then be readily compared with the RO results. The terms $\mathcal{F}_0(\hat{P}_t^X)$ and $\mathcal{F}_h(\hat{P}_t^X)$ are obtained by substituting (66) in (2), executing the affine and non-affine operations, and separating the center and radius terms. Note that the noise of the non-affine terms in (63) are assumed to be -1 in the objective function, since, as previously explained, these non-affine terms are internal source of errors, and thus this minimizes the conservative internal error associated with the non-affine terms, so as not to obtain a large uncertainty radius.

Constraints in Section II can then be written in their AA form according to (61) and (62). Thus, the inter-temporal constraint

(12) can be formulated as follows:

$$SOC_{0,t+1} = SOC_{0,t} + \frac{(air^C_{0,t} - air^D_{0,t})3600}{\overline{CA}} \qquad \forall t \tag{68}$$

$$\sum_{h=1}^{p} SOC_{h,t+1} = \sum_{h=1}^{p} SOC_{h,t} + \sum_{h=1}^{p}\left[\frac{(air^C_{h,t} - air^D_{h,t})3600}{\overline{CA}}\right] \qquad \forall t \tag{69}$$

$$SOC_{0,t+1} - \sum_{h=1}^{p} |SOC_{h,t+1}| \geq SOC^f \qquad \forall t = T \tag{70}$$

where (68) and (69) denotes the center and radius of the SOC, respectively. Note that the equality of noise symbols is not guaranteed in (69), but it assures that no operating limits are violated. To be able to better participate in the electricity market the next day, (70) guarantees that the SOC at the end of the day will be at least equal to SOC^f.

The proposed AA model determines the center and radius, i.e., it provides an interval of the daily profit and power dispatches. Hence, if the price mismatch at hour t is known, then the noise term can be readily calculated, which allows to determine the power dispatch and profit values corresponding to the known errors in prices, thus yielding single values for these variables.

V. Results and Discussions

For simulation, validation, and comparison purposes, the CAES facility is assumed to have a maximum charging and discharging of 60 MW and 100 MW, respectively, while the minimum charging and discharging are 25 MW and 30 MW, respectively, and a quick start capacity of 40 MW, as per [10]. To operate within the pressure limits, the SOC of the cavern is maintained between 33% to 100% as in [10]. For all simulations carried out, the initial and final SOC of the facility was assumed to be 60%. The maximum mass of air the cavern can store is assumed to be the amount of air the cavern would discharge if operated at full power for eight straight hours. Electricity prices are taken from the Ontario electricity market historical data [29]. The simulations were executed for two different volatile days denoted as Day 1 (February 6, 2019) and Day 2 (January 19, 2019, which is less volatile), with different price profiles depicted in Fig. 3. All simulations were performed in GAMS interfaced with MATLAB.

A. Comparison Between Thermodynamic Models

To validate and evaluate the performance of the proposed linear thermodynamic model, the results obtained for the deterministic case are compared with the CAES model of [10], where the thermodynamic characteristics of the facility are represented by step functions. Thus, Table I presents a comparison of the profit and computational costs for the proposed linear model

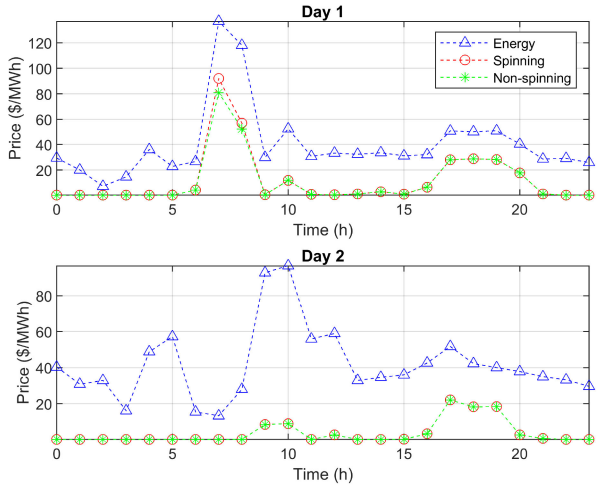

Fig. 3. Prices profile for Days 1 and 2.

TABLE I
Comparison Between Linear and Step Models

		Linear Model	Step Model [10]
Day 1	Profit ($)	30,919	30,932
	Computing Time	1.23s	28min42s
Day 2	Profit ($)	25,349	25,617
	Computing Time	1.17s	2min58s

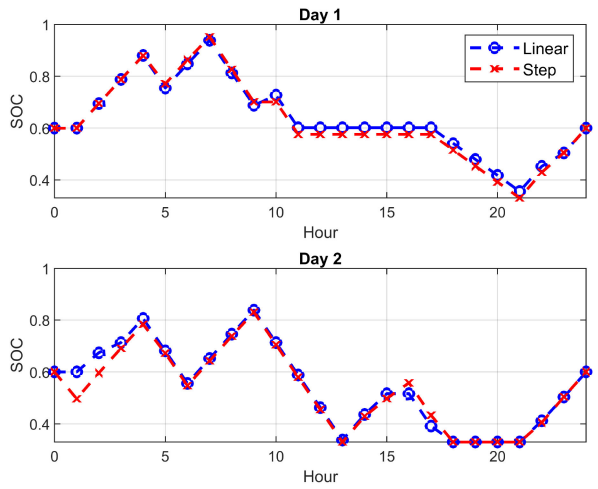

Fig. 4. SOC comparison of the Linear and Step models.

compared to the model in [10], which are denoted as Linear and Step Models, respectively. Note that both methodologies yield similar profits, with a maximum mismatch of 1%, but the Linear Model is much faster computationally. Thus, for both days, the Linear Model converged in seconds, while the Step Model took much longer, with significant solution time differences between Day 1 to Day 2, which suggests that the Step Model computational performance be quite sensitive to price input data.

Fig. 4 presents the optimum schedule obtained from each model for both days. Note that the optimum schedules are very similar throughout the day for both models.

TABLE II
CAES PROFIT FOR ROBUST OPTIMIZATION ($)

Γ	Day 1			Day 2		
	8%	15%	20%	8%	15%	20%
0	30,919	30,919	30,919	25,349	25,349	25,349
5	27,484	24,566	22,482	22,236	19,592	17,704
10	26,908	23,481	21,057	21,028	17,436	14,927
15	26,649	23,159	20,677	20,505	16,566	13,876
20	26,649	23,159	20,677	20,374	16,317	13,876
24	26,649	23,159	20,677	20,374	16,317	13,876

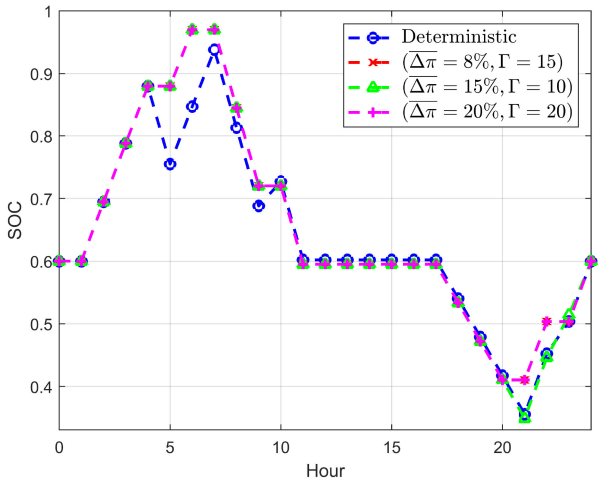

Fig. 5. Day 1 SOC for different $\overline{\Delta\pi}$ and Γ.

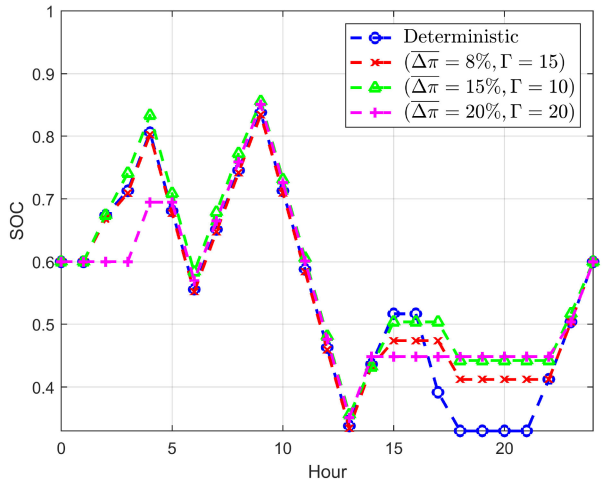

Fig. 6. Day 2 SOC for different $\overline{\Delta\pi}$ and Γ.

TABLE III
PROBABILITY OF VIOLATION

Γ	0	5	10	15	20	24
p [%]	58.09	20.71	3.31	0.21	5.26e-3	1.33e-4

TABLE IV
CAES PROFIT FOR AFFINE ARITHMETIC ($)

$\overline{\Delta\pi}$	Day 1			Day 2		
	Lower	Center	Upper	Lower	Center	Upper
8%	17,065	27,000	36,936	8,961	20,555	32,149
15%	15,409	28,416	41,422	8,996	22,697	36,397
20%	12,604	28,704	44,877	6,538	23,235	39,932

B. Robust Optimization Results

For each day, the simulations of the RO were carried out for different values of $\overline{\Delta\pi}$ and Γ, assuming for each parameter the following values: $\overline{\Delta\pi} \in$ [8%,15%,20%], and $\Gamma \in$ [0,5,10,15,20,24]. Thus, 18 scenarios were simulated for each day.

Table II presents the daily profit for the CAES facility for each day, for different combinations of $\overline{\Delta\pi}$ and Γ. For $\Gamma = 0$, which is the deterministic case, the profits for different values of $\overline{\Delta\pi}$ do not change. As Γ increases, the number of times the prices deviate from their forecast increases, and consequently, the profits decrease. Also, the sensitivity of profit reduces as Γ tends to the most conservative scenario, i.e., $\Gamma = 24$. As expected, greater values of $\overline{\Delta\pi}$ lead to lower profits. Note also that the facility's profit on Day 1 are generally higher than on Day 2, which can be attributed to the overall higher market price profile on Day 1, as shown in Fig. 3.

As prices deviate from their forecast values, the optimum daily schedule is susceptible to changes. Thus, in Fig. 5 and Fig. 6 the SOC for different combinations of $\overline{\Delta\pi}$ and Γ for Day 1 and Day 2, respectively, are presented; for both days, it can be observed that in the deterministic scenario the facility charges and discharges more, whereas for the scenarios with uncertainties, the facility is more conservative, operating in idle mode for more hours, as expected.

As presented in (51), for each Γ there is a probability of violation p given in Table III. Note that a higher financial protection level, i.e., a low value of p, is achieved in less conservative scenarios, i.e., for low values of Γ; for instance, $\Gamma = 10$ yields a probability of violation lower than 5%.

C. Affine Arithmetic Results

For the proposed AA model, simulations were carried out to maximize the center and the radius of the profit simultaneously, as per (67). Since there are no parameters to control the level of conservatism, AA obtains a single optimum interval schedule for each $\overline{\Delta\pi}$.

Table IV presents the center, upper and lower bounds of the profit for each day. Observe that as $\overline{\Delta\pi}$ increases, the center and radius of the profit increases, i.e., a larger difference can be seen between the upper and lower bounds with respect to the center value, as expected.

For different $\overline{\Delta\pi}$, the optimum daily schedules of the facility are sensitive to changes, as illustrated in Fig. 7 and Fig. 8. Note that the SOC solution is an interval, as expected; depending on the magnitude of $P^C_{h,t}/P^D_{h,t}$, the SOC have tighter or larger intervals. Compared with the deterministic schedule, observe that the dispatch decisions are similar most of the time but with different Depth of Discharge (DoD).

When operating the CAES facility, the power dispatch variables need to be obtained from the intervals computed with the AA model. Thus, when the actual price mismatch with respect

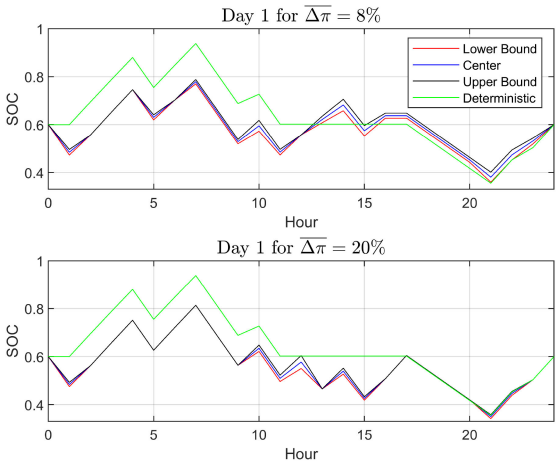

Fig. 7. Day 1 SOC for different $\overline{\Delta\pi}$.

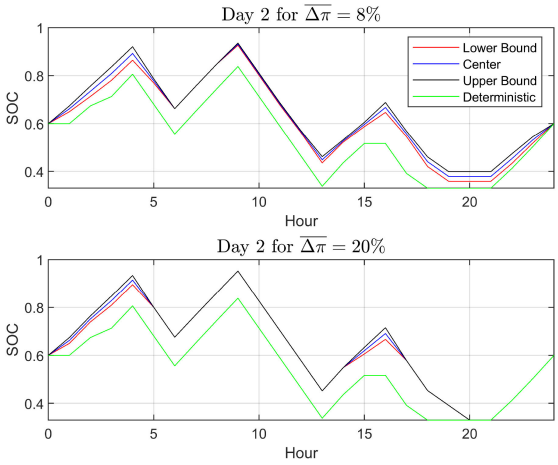

Fig. 8. Day 2 SOC for different $\overline{\Delta\pi}$.

to the forecasted center value ε_t^Y is known, the power dispatch of the facility can be determined. For example, assuming that the CAES facility is following the optimum schedule obtained from $\overline{\Delta\pi} = 8\%$ in Day 1, and that for $t = 2\ h$ the facility is discharging, for a mismatch of -5% in the energy price and no mismatches in the other prices, the noise values can be determined to be $\varepsilon_t^E = -\frac{5\%}{8\%} = -0.625$, $\varepsilon^{SR} = 0$ and $\varepsilon^{ID} = 0$. Thus, the SOC at t can then be computed to be $SOC_2 = 0.464$. If the mismatch is lower than -8% or greater than 8%, ε_t^E can be set to -1 or 1, respectively.

D. Comparisons

To validate the results obtained from RO and AA, both are compared here with the MCS approach, assuming uniform pdfs. Thus, three random uniform distributions were generated, each with a thousand data points. The MCS results for the uniform pdfs with the ranges of [0.92,1.08], [0.85,1.15], and [0.8,1.2] for the three market prices were compared with the RO and AA, for $\overline{\Delta\pi}$ of 8%, 15%, and 20%, respectively.

Fig. 9 presents a comparison between the MCS, AA and RO, for both days, depicting the upper and lower bounds of

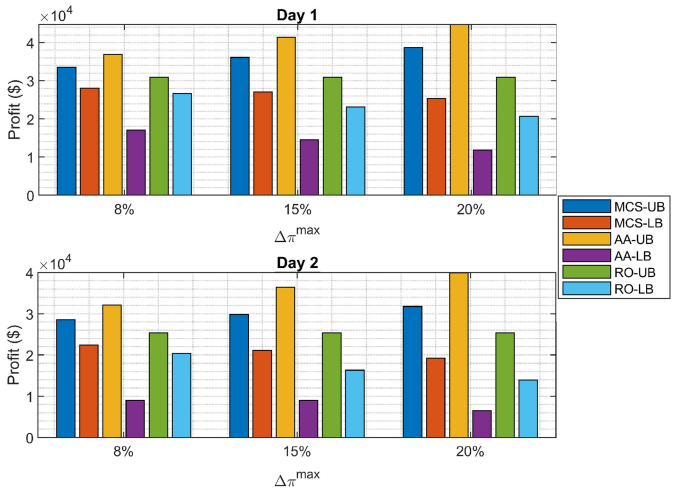

Fig. 9. MCS, AA and RO comparison.

the MCS (MCS-UB and MCS-LB, respectively), AA (AA-UB and AA-LB) and RO (RO-UB and RO-LB). For RO, the upper and lower bounds corresponds to the results of the deterministic case and the most conservative scenario, i.e., $\Gamma = 0$ and $\Gamma = 24$, respectively. Observe for both days and all values of $\overline{\Delta\pi}$ that the AA solution profile envelops both the MCS and RO solutions. Since the RO objective is to optimize the profit for the worst-case scenario, its profits are higher in the lower bound, as compared to AA. The MCS approach incurs the highest computational burden while RO has the lowest, converging in a few seconds. Since a large number of variables are used to keep track of the correlated uncertainties, the AA approach has a larger computational burden than RO; however, it still converges in a few seconds. Therefore, given a $\overline{\Delta\pi}$ which the CAES facility seeks to be protected from, the plant operator determine the optimum schedule using either RO or AA. If RO is employed, given the probabilities of violation in Table III, the operator choose a schedule with the desired protection level. However, if AA is used, there is a unique optimum schedule, where, given the real-time mismatch in prices, the power dispatches of the facility can be determined.

E. Effects of Different SOC Levels

In this section, the impact of the initial and final SOC^f value of the CAES facility optimal operation is analyzed. Since electricity prices are usually lower at the early hours of the day, the facility typically starts the day by charging and reaching a high value of SOC, and when prices increase it starts discharging. Thus, a higher initial SOC would yield a conservative schedule wherein the range of operation will be constrained. If the final SOC is held at a relatively high value, then the facility would not have a high DoD, resulting in low profits. Therefore, different initial and final SOC levels are tested here using the price profile of Day 1, to demonstrate the impact of the SOC^f value on profits and optimum daily schedules.

Table V presents the profits of the CAES facility using the RO approach for values of SOC^f equal to 0.7 (70% SOC) and 0.8

TABLE V
CAES PROFIT FOR RO FOR DAY 1 ($)

Γ	$SOC^f = 0.7$			$SOC^f = 0.8$		
	8%	15%	20%	8%	15%	20%
0	30,676	30,676	30,676	29,952	29,952	29,952
5	27,157	24,143	22,075	26,440	23,415	21,311
10	26,547	23,076	20,710	25,828	22,325	19,925
15	26,287	22,776	20,286	25,502	21,941	19,652
20	26,287	22,776	20,286	25,502	21,941	19,652
24	26,287	22,776	20,286	25,502	21,941	19,652

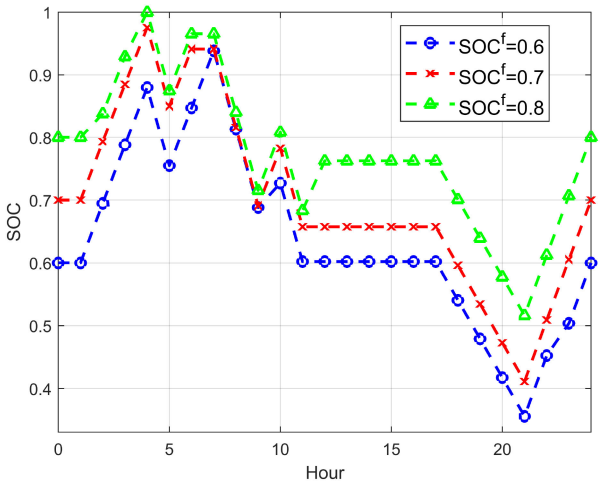

Fig. 10. Deterministic schedule for Day 1.

TABLE VI
CAES PROFIT FOR AA FOR DAY 1 ($)

$\overline{\Delta\pi}$	$SOC^f = 0.7$			$SOC^f = 0.8$		
	Lower	Center	Upper	Lower	Center	Upper
8%	17,083	26,840	36,597	16,946	26,463	35,979
15%	14,912	28,022	41,131	14,414	27,506	40,598
20%	12,467	28,533	44,599	12,410	28,260	44,111

(80% SOC). When compared to Table II, which used an initial SOC of 60%, note that the profits from the deterministic schedule ($\Gamma = 0$) to the most conservative scenario ($\Gamma = 24$) decrease for higher levels of SOC^f, for all price mismatch scenarios. Fig. 10 illustrates the optimum deterministic schedule for the CAES facility for different values of SOC^f. Observe that when $SOC^f = 0.6$, the CAES facility operates with a larger DoD as compared to the cases with initial and final SOCs of 70% and 80%.

Table VI depicts the CAES facility profits using the AA approach for different SOC^f values. Observe that the center, lower, and upper boundaries of the profit profile decrease for higher values of initial and final SOC, as expected, since the interval of operation is tighter, as shown in Fig. 11. Note that compared to the deterministic schedule, the dispatch decisions remain similar but with different DoDs. Therefore, operating with high SOC^f values is not advantageous for the CAES facility, since it yields conservative schedules and profits to ensure that the desired final SOC value is met at the end of the day, thus missing opportunities to maximize the daily profit.

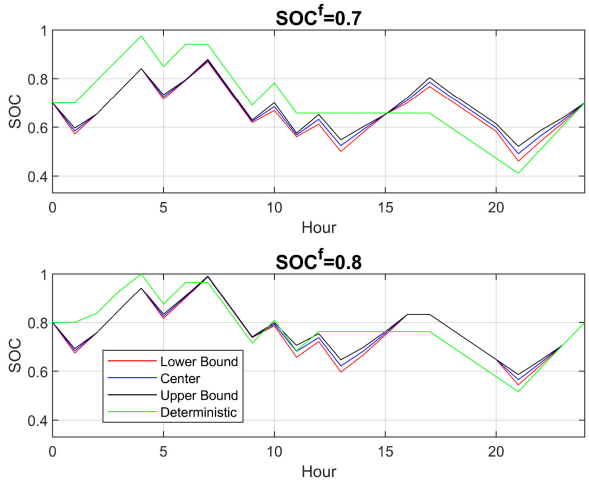

Fig. 11. AA schedule for $\overline{\Delta\pi} = 8\%$ for Day 1.

VI. CONCLUSION

This paper presented RO and AA-based self-scheduling models to maximize the daily profit of a price-taker CAES facility under price uncertainties, considering its thermodynamic characteristics. The RO model presented the lowest computational burden and the simulations yielded multiple possible schedules, from which the operator has to choose an appropriate one based on the budget of uncertainty. In AA, despite a higher computational burden, an optimum schedule was obtained, with the center value and the radius of the bounds of the profit and power dispatch variables. For validation purpose, both methods were compared with the MCS approach, showing that both methods were computationally faster than the MCS, while also capturing a wider interval range of results. For future work, the authors intend to examine the operation of a CAES facility as a price-maker, using both RO and AA to model the uncertainties in RES generation, load, and bids/offers of the market participants.

REFERENCES

[1] G. T. Heydt, "Grand challenges in electric power engineering: Extreme system reliability," in *Proc. IEEE Power Eng. Soc. Summer Meeting*, Jul. 2002, pp. 1695–1697.
[2] A. A. Akhil *et al.*, "DOE/EPRI 2013 electricity storage handbook in collaboration with NRECA," Sandia Nat. Lab., Albuquerque, New Mexico, Jul. 2013. [Online]. Available: https://www.energy.gov/sites/prod/files/2013/08/f2/ElecStorageHndbk2013.pdf
[3] J. Arteaga and H. Zareipour, "A price-maker/price-taker model for the operation of battery storage systems in electricity markets," *IEEE Trans. Smart Grid*, vol. 10, no. 6, pp. 6912–6920, Nov. 2019.
[4] N. Padmanabhan, M. Ahmed, and K. Bhattacharya, "Battery energy storage systems in energy and reserve markets," *IEEE Trans. Power Syst.*, vol. 35, no. 1, pp. 215–226, Jan. 2020.
[5] H. Alharbi and K. Bhattacharya, "Participation of pumped hydro storage in energy and performance-based regulation markets," *IEEE Trans. Power Syst.*, vol. 35, no. 6, pp. 4307–4323, Nov. 2020.
[6] B. J. Davidson *et al.*, "Large-scale electrical energy storage," *IEE Proc. A. - Phys. Sc., Meas. Instrum., Manage. Educ. - Rev.*, vol. 127, no. 6, pp. 345–385, 1980.
[7] T. V. Nguyen, "Integration of compressed air energy storage with wind turbine to provide energy source for combustion turbine generator," in *Proc. IEEE PES Innov. Smart Grid Technol.*, Eur., 2014, pp. 1–5.

[8] "Goderich A-CAES facility," Hydrostor, 2020. [Online]. Available: https://www.hydrostor.ca/goderich-a-caes-facility
[9] I. Calero, C. A. Cañizares, and K. Bhattacharya, "Compressed air energy storage system modeling for power system studies," *IEEE Trans. Power Syst.*, vol. 34, no. 5, pp. 3359–3371, Sep. 2019.
[10] S. Shafiee, H. Zareipour, and A. M. Knight, "Considering thermodynamic characteristics of a CAES facility in self-scheduling in energy and reserve markets," *IEEE Trans. Smart Grid*, vol. 9, no. 4, pp. 3476–3485, Jul. 2018.
[11] S. Shafiee, H. Zareipour, A. M. Knight, N. Amjady, and B. Mohammadi-Ivatloo, "Risk-constrained bidding and offering strategy for a merchant compressed air energy storage plant," *IEEE Trans. Power Syst.*, vol. 32, no. 2, pp. 946–957, Mar. 2017.
[12] S. Nojavan, A. Najafi-Ghalelou, M. Majidi, and K. Zare, "Optimal bidding and offering strategies of merchant compressed air energy storage in deregulated electricity market using robust optimization approach," *Energy*, vol. 142, pp. 250 – 257, 2018. [Online]. Available: http://www.sciencedirect.com/science/article/pii/S0360544217316973
[13] A. Attarha, N. Amjady, S. Dehghan, and B. Vatani, "Adaptive robust self-scheduling for a wind producer with compressed air energy storage," *IEEE Trans. Sustain. Energy*, vol. 9, no. 4, pp. 1659–1671, Oct. 2018.
[14] K. Sundar, H. Nagarajan, L. Roald, S. Misra, R. Bent, and D. Bienstock, "Chance-constrained unit commitment with n-1 security and wind uncertainty," *IEEE Control Netw. Syst.*, vol. 6, no. 3, pp. 1062–1074, Sep. 2019.
[15] M. H. Ahmed, K. Bhattacharya, and M. M. A. Salama, "Analysis of uncertainty model to incorporate wind penetration in LMP-based energy markets," in *Proc. 2nd Int. Conf. Elect. Power Energy Convers. Syst.*, Nov. 2011, pp. 1–8.
[16] J. D. Lara, D. E. Olivares, and C. A. Cañizares, "Robust energy management of isolated microgrids," *IEEE Syst. J.*, vol. 13, no. 1, pp. 680–691, Mar. 2019.
[17] S. Shafiee, H. Zareipour, and A. M. Knight, "Developing bidding and offering curves of a price-maker energy storage facility based on robust optimization," *IEEE Trans. Smart Grid*, vol. 10, no. 1, pp. 650–660, Jan. 2019.
[18] A. Vaccaro, C. A. Cañizares, and D. Villacci, "An affine arithmetic-based methodology for reliable power flow analysis in the presence of data uncertainty," *IEEE Trans. Power Syst.*, vol. 25, no. 2, pp. 624–632, May 2010.
[19] M. Pirnia, C. A. Cañizares, K. Bhattacharya, and A. Vaccaro, "A novel affine arithmetic method to solve optimal power flow problems with uncertainties," *IEEE Trans. Power Syst.*, vol. 29, no. 6, pp. 2775–2783, Nov. 2014.
[20] D. Romero-Quete and C. A. Cañizares, "An affine arithmetic-based energy management system for isolated microgrids," *IEEE Trans. Smart Grid*, vol. 10, no. 3, pp. 2989–2998, May 2019.
[21] A. Vaccaro, M. Petrelli, and A. Berizzi, "Robust optimization and affine arithmetic for microgrid scheduling under uncertainty," in *Proc. IEEE Int. Conf. Environ. Elect. Eng. Ind. Commercial Power Syst. Eur.*, 2019, pp. 1–6.
[22] H. Zareipour, A. Janjani, H. Leung, A. Motamedi, and A. Schellenberg, "Classification of future electricity market prices," *IEEE Trans. Power Syst.*, vol. 26, no. 1, pp. 165–173, Feb. 2011.
[23] A. O. Abani, N. Hary, M. Saguan, and V. Rious, "Risk aversion and generation adequacy in liberalized electricity markets: Benefits of capacity markets," in *Proc. 13th Int. Conf. Eur. Energy Market*, 2016, pp. 1–5.
[24] Y. Li *et al.*, "A real-time dispatch model of CAES with considering the part-load characteristics and the power regulation uncertainty," *Int. J. Elect. Power Energy Syst.*, vol. 105, pp. 179 – 190, 2019. [Online]. Available: http://www.sciencedirect.com/science/article/pii/S0142061518314650
[25] A. Costa and L. Liberti, "Relaxations of multilinear convex envelopes: Dual is better than primal," in *Proc. Int. Symp. Exp. Algorithms*, 2012, pp. 87–98.
[26] D. Bertsimas and M. Sim, "The price of robustness," *Oper. Res.*, vol. 52, no. 1, pp. 35–53, 2004.
[27] J. Stolfi and L. H. de Figueiredo, "Self-validated numerical methods and applications," in *Proc. 21st Brazilian Math. Colloq. (IMPA)*, Rio de Janeiro, Brazil, 1997. [Online]. Available: http://www-sbras.nsc.ru/interval/Library/InteBooks/Stolfi.pdf
[28] A. Vaccaro and C. A. Cañizares, "An affine arithmetic-based framework for uncertain power flow and optimal power flow studies," *IEEE Trans. Power Syst.*, vol. 32, no. 1, pp. 274–288, Jan. 2017.
[29] "M. prices," IESO. [Online]. Available: http://reports.ieso.ca/public/PriceHOEPPredispOR/

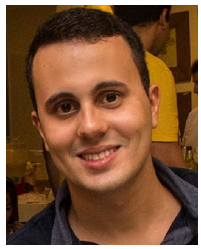

Matheus F. Zambroni de Souza received the Diploma and master's degree in electrical engineering from Universidade Federal de Itajuba, Itajuba, Brazil, in 2015 and 2017, respectively. He is currently working toward the Ph.D. degree in electrical engineering with the University of Waterloo, Waterloo, ON, Canada. He had experience working with power systems stability during his undergraduation and power quality and signal processing during his master's. His current research focuses on compressed air energy storage participation in the electricity market, using robust optimization and/or affine arithmetic to model uncertainties.

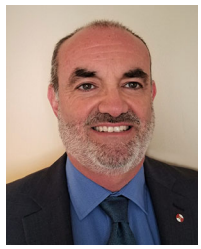

Claudio A. Cañizares (Fellow, IEEE) is currently a University Professor and the Hydro One Endowed Chair with the ECE Department, University of Waterloo, Waterloo, ON, Canada, where he has been since 1993. His current research interests include modeling, simulation, computation, stability, control, and optimization of power and energy systems. He is with the IEEE TRANSACTIONS ON SMART GRID EIC, the PES Delegate-Elect to the IEEE Board, the Royal Society of Canada, and the Canadian Academy of Engineering. He was the recipient of the 2017 IEEE PES Outstanding Power Engineering Educator Award, the 2016 IEEE Canada Electric Power Medal, and multiple awards and recognitions from PES Technical Committees.

Kankar Bhattacharya (Fellow, IEEE) received the Ph.D. degree in electrical engineering from the Indian Institute of Technology Delhi, New Delhi, India, in 1993. He was with the Faculty of Indira Gandhi Institute of Development Research, Mumbai, India, from 1993 to 1998, and with the Department of Electric Power Engineering, Chalmers University of Technology, Gothenburg, Sweden, from 1998 to 2002. In 2003, he joined Electrical and Computer Engineering Department, University of Waterloo, Waterloo, ON, Canada, where he is currently a Full Professor. His current research interests include power system economics and operational aspects. He is a Registered Professional Engineer in the province of Ontario.